J Solid State Eletrochem (2004) 8: 218–223
DOI 10.1007/s10008-003-0469-6

ORIGINAL PAPER

S. Franger · P. Berthet · J. Berthon

Electrochemical synthesis of Fe_3O_4 nanoparticles in alkaline aqueous solutions containing complexing agents

Received: 29 July 2003 / Accepted: 29 September 2003 / Published online: 13 February 2004

Abstract Ultrafine magnetite particles are prepared through an electrochemical process, at room temperature, from an iron-based electrode immersed in an alkaline aqueous medium containing complexing compounds. XRD and chemical analysis indicate that the product is pure magnetite, Fe_3O_4. The size and morphology of the particles are studied by SEM. The magnetite nanoparticles present a magnetoresistance of almost 3%, at 300 K, under a magnetic field of 1 T. A reactive mechanism for the electrochemical process is proposed.

Keywords Inorganic electrosynthesis · Iron oxide · Iron(III) oxyhydroxide · Magnetite · Nanoparticles

Introduction

Magnetite (Fe_3O_4) has natural magnetic properties that provide a multitude of uses in industry. The quality of magnetite used has been particularly important to the magnetic recording industry. With the demand for smaller and lighter-weight magnetic recording devices, there has been an increasing need for recording media (such as magnetic recording tape and magnetic disks, for example) to have a higher recording density and sensitivity. In order to meet these demands, the magnetite particles produced would desirably have a smaller particle size with a higher coercive force.

Currently, chemical processes are employed to produce magnetite: coprecipitation of both iron(II) and iron(III) salts in alkaline aqueous solution [1, 2, 3, 4, 5, 6, 7], oxidation of iron(II) hydroxide with an alkaline nitrate or oxygen [7, 8], or reduction, at high temperature, of γ-Fe_2O_3 by means of a CO/CO_2 or a hydrogen gas flow [9, 10]. We can also cite recent investigations towards hydrothermal processes in different aqueous or non-aqueous solvents [7, 11, 12, 13, 14, 15, 16]. Although these chemical routes are known to produce magnetite, such processes typically produce relatively large-sized particles having a low coercive force. In addition, the aforementioned chemical techniques tend to produce magnetite with a relatively high impurity content. Accordingly, the optimal characteristics of magnetite recording materials are not fully realized as a result of the undesirable characteristics encountered by these current practices.

The electrochemical synthesis presented here produces pure, homogeneous, nano-sized particles of magnetite. Different physicochemical parameters are studied in order to first understand the mechanism of the reaction and then to optimize the conditions of the electrosynthesis.

S. Franger (✉) · P. Berthet · J. Berthon
Laboratoire de Physico-Chimie de l'Etat Solide,
UMR CNRS 8648, Université Paris XI, 91405 Orsay, France
E-mail: sylvain.franger@lpces.u-psud.fr
Tel.: +33-1-69156312
Fax: +33-1-69154797

Experimental

Preparation of the magnetite nanoparticles

Electrochemical studies were carried out in classical three-electrodes cells. The working electrode (WE) consisted of a stainless steel pellet (Y45, free of nickel or chromium) with a geometric area of 4 cm^2. The counter electrode (CE) was a platinum wire and the reference was a saturated calomel electrode, SCE ($E_{ref} = 0.24$ V/SHE).

Different aqueous electrolytes were studied for the electrosynthesis of magnetite: 0.04 mol L^{-1} (Na^+, Cl^-), 0.02 mol L^{-1} ($2Na^+$, SO_4^{2-}), 0.02 mol L^{-1} (Na^+, SCN^-), 0.02 mol L^{-1} ($2Na^+$, $S_2O_3^{2-}$) and 0.003 mol L^{-1} ($3Na^+$, Cit^{3-}), where $\{Cit^{3-}\}$ represents structure **1**. The different salts (obtained from Fluka) were dissolved in deionized water and the pH was then fixed at 10 with concentrated sodium hydroxide solution.

Galvanostatic measurements (performed at 50 mA) were made with a Heathkit L.V. Power Supply (model IP-27). A.c. impedance measurements were made, in the frequency range 3×10^4 to 5 Hz, with an HP 4192A apparatus driven by an IBM computer. The excitation signal was 15 mV peak-to-peak with a voltage bias fixed at 5 V between working and counter electrodes. The equivalent

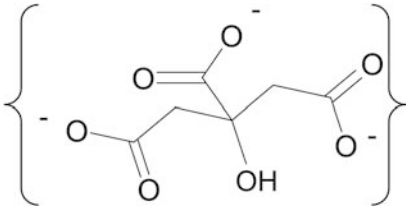

circuits were modelled by a series of resistance and constant phase element (CPE) loops [17, 18], whose values were obtained by the software Zplot (Scribner Associates).

Characterization of the samples

The mean oxidation state of iron was determined by double chemical titration. Actually, two powder samples were dissolved in an aqueous solution containing 50% (v/v) concentrated H_2SO_4. The first sample was directly titrated with an acidic solution of $K_2Cr_2O_7$ in the presence of sodium diphenylaminesulfonate as an indicator [19]. This experiment leads to the amount of Fe^{2+} ions. The second sample was completely reduced with an excess of aluminium metal powder [20]. When all iron(III) ions have vanished (a rapid control test with KSCN can easily be performed to ensure that the entire reduction was done), the solution was filtered and titrated as previously reported [19], which gives the total amount of iron. The accuracy of this chemical titration method is $\pm 2\%$.

XRD experiments were performed with a Philips PW 3020 diffractometer using Cu $K_{\alpha 1}$ radiation ($\lambda = 1.54056$ Å). Particle size information was obtained from X-ray diffraction line broadening and electron microscopy (SEM). Electron micrographs confirmed that the particles were roughly spherical and allowed us to determine the mean coherence length distribution using the Scherrer equation [21]:

$$d = \frac{0.89\lambda}{\beta \cos\theta} \quad (1)$$

where λ is the wavelength of radiation, β is the line broadening (in radians), θ is the angle of diffraction and d is the mean coherence length.

The thermogravimetric analysis (TGA) was made with a Setaram 92-16.18 analyzer. The magnetoresistance (MR) at grain boundaries was measured by the four-probe d.c. conductivity method [22] with a SQUID magnetometer (Quantum Design MPMS-5), at room temperature (300 K), under magnetic fields ≤ 1 T. The tested sample consisted of Fe_3O_4 powder, used as synthesized, just pressed at 4×10^3 kg cm^{-2} during 10 min, without any thermal treatment.

Results and discussion

The open circuit voltage (OCV) of the stainless steel electrodes in the different alkaline electrolytes was recorded during 5 min to check the stability and reliability of the initial surface state of the iron samples. Measurements in solutions each containing complexing entities were quite reproducible. The obtained values are reported in Table 1.

The experimental conditions, a narrow range of potentials around the OCV, are such that the elementary anodic electrochemical process should be:

$$Fe + 3OH^- \rightleftharpoons \gamma\text{-}FeOOH + 3e^- \quad (2)$$

whose standard thermodynamic potential is [23]:

Table 1 Open circuit voltage of stainless steel electrodes in different aqueous electrolytes (pH 10)

Complexing agent in electrolyte	OCV (V/SCE)
Cl^-	−0.790
SO_4^{2-}	−0.770
$S_2O_3^{2-}$	−0.785
SCN^-	−0.780
Cit^{3-}	−0.770

$$E^o_{\gamma-FeOOH/Fe} = 0.042 - 0.059\ pH \quad V/SHE \quad (3)$$

i.e.:

$$E^o_{\gamma-FeOOH/Fe} = -0.788/SCE \ \text{ at } \ pH = 10 \quad (4)$$

The potentials obtained are very close to the theoretical value. The small differences could be assigned to kinetic parameters involved in the corrosion process.

As soon as a constant current (50 mA) is applied between the counter and working electrodes, the WE potential increases due to solid formation of small yellow-brown particles at the iron metal surface (except when the electrolyte used was citrate, where no solid formation was noticed). This reaction occurs parallel to the production of dihydrogen gas on platinum. Chemical analysis of these fine and homogeneous particles was made and confirmed, unsurprisingly, the formation of iron(III) oxyhydroxide (lepidocrocite).

The formation of magnetite seems not to be predominant in our experimental conditions. However, after several minutes of anodic polarization of the iron-based working electrode and the stabilization of its potential due to coalescence of the particles onto the WE, a quantitative amount of Fe_3O_4 is observed (except in citrate electrolyte) (Fig. 1) and the colloidal solution turns from yellow-brown to black more or less rapidly (depending on the complexing salts employed, Fig. 2).

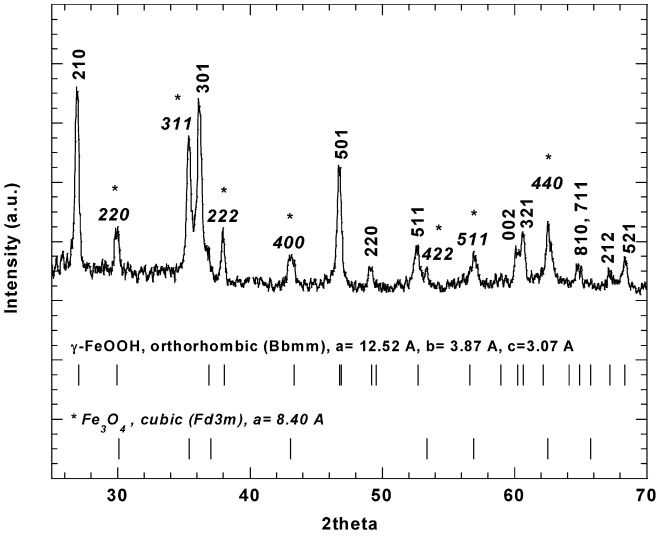

Fig. 1 An example of XRD patterns obtained when the first black particles of magnetite begin to appear

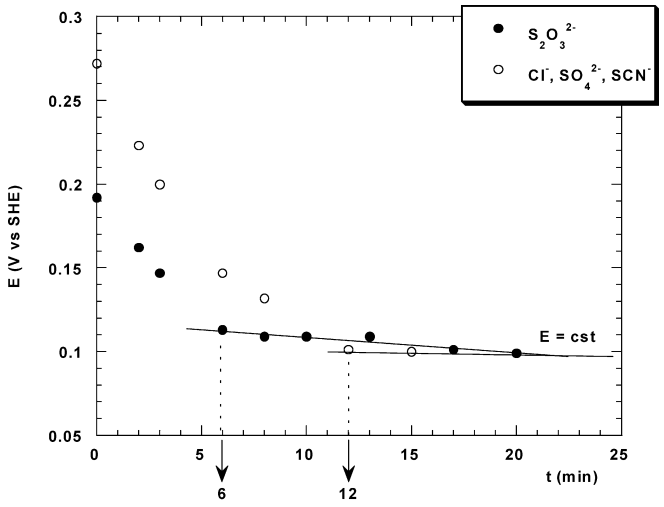

Fig. 2 Influence of the nature of the complexing agent on the time to observe the first black particles of magnetite

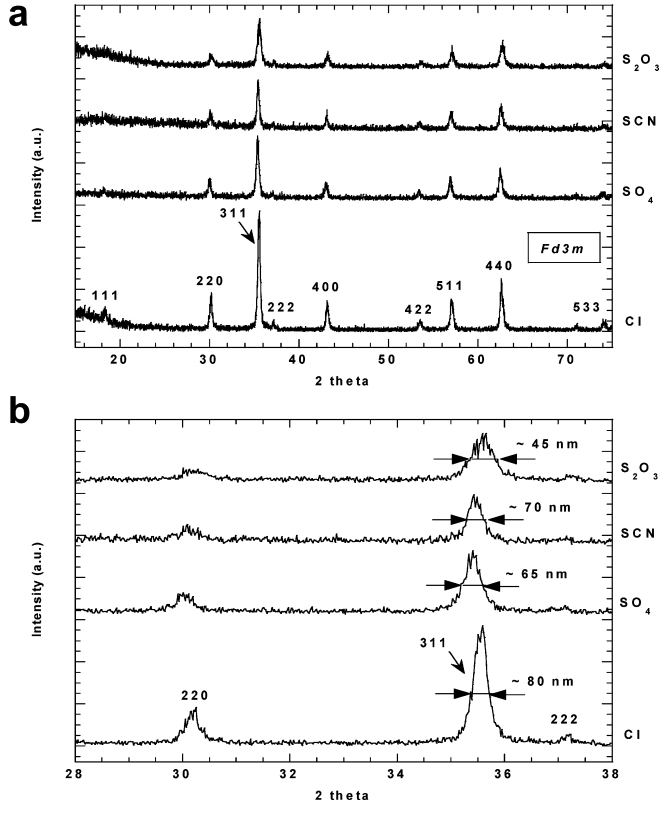

Fig. 3 (**a**) XRD patterns of magnetite as a function of the nature of the complexing agent; (**b**) a view between 28° and 38° (2θ), with the calculated mean coherence length

After 30 min, the analysis of the electrosynthesized particles always confirmed the formation of pure magnetite.

All XRD patterns can be indexed in the cubic system (*Fd*3*m*) and we do not observe any parasitic peaks due to impurities (Fig. 3a). The line broadening indicates that the particles are very small. Depending on the electrolyte used, the mean coherence length is between 45 and 80 nm (calculated with Eq. 1 from XRD diagrams, Fig. 3b and Table 2).

SEM micrography performed on a sample of magnetite confirmed the nanometer scale of the particles (Fig. 4) and the size observed (Ø≈82 nm) is consistent with the precedent mean coherence length calculated from corresponding XRD patterns (Table 2).

TGA experiments (Fig. 5) were carried out, under air, between room temperature and 300 °C. The weight loss between ambient to 100 °C can be ascribed to water desorption, following the reaction:

$$\begin{aligned} Fe_3O_4 \cdot xH_2O \;&\rightarrow\; Fe_3O_4 + xH_2O \\ (\Delta m)_{exp} &= -2.5\% \end{aligned} \tag{5}$$

We can then calculate the amount of water molecules adsorbed onto the surface of the particles. The result gives the following general molecular formula: $Fe_3O_4.0.33H_2O$. Such an amount of non-stoichiometric water molecules is frequent in materials synthesized in aqueous media [24]. The hypothesis of adsorption is made regarding the XRD patterns (Fig. 3a). As no peak shift towards higher angles is observed in our samples compared to theoretical patterns, it means that the water cannot be intercalated into the structure like for layered transition metal oxides (δ-MnO_2, for example) [25, 26].

Between 100 °C and 300 °C, the weight gain is ascribed to the oxidation of the compound as follows:

$$\begin{aligned} 2Fe_3O_4 + {}^1\!/_2O_2 \;&\rightarrow\; 3\gamma - Fe_2O_3 \\ (\Delta m)_{th} = 1.7\% \quad &(\Delta m)_{exp} = 1.4\% \end{aligned} \tag{6}$$

This phase transition is well described in the literature [27, 28] and corresponds to the transformation of magnetite into maghemite, which can also be seen by an X-ray diffraction experiment (Fig. 6).

The molecular formula being defined, a chemical titration can be performed on each compound (Table 2). The ratio iron(II)/iron(III) is respected for all samples whatever the electrolyte used (except for citrate, which does not allow the synthesis of Fe_3O_4).

In order to understand the mechanism of magnetite formation in these different media, we then performed several complementary experiments. First, we changed the place of the cathode (the platinum wire) in the electrochemical cell. The conclusion is that the synthesis of Fe_3O_4 is very dependent of the place of the counter electrode, since the farther away it is, the longer is the time to observe the first black particles of magnetite; at extremum, when the platinum wire is in a separate vessel, no Fe_3O_4 is produced (Fig. 7).

The dihydrogen present at the counter electrode should have an important role in the formation of magnetite. Indeed, its diffusion through the solution allows us to reduce partially the iron(III) oxyhydroxide particles formed at the working electrode.

The EC mechanism can be described by the following elementary reactions:

Table 2 Ratio of iron(II)/iron(III) (determined by chemical titration), lattice parameter of the cubic Fe_3O_4 structure and mean coherence length of the crystallites (calculated using XRD patterns and Eq. 1) as a function of the electrolytes used

Complexing agent in electrolyte	Ratio Fe(II)/Fe(III)	Lattice parameter, a (Å)	Mean coherence length (nm)
Cl^-	0.49	8.39	~80
SO_4^{2-}	0.50	8.40	~65
$S_2O_3^{2-}$	0.50	8.38	~45
SCN^-	0.49	8.39	~70
Cit^{3-}	No Fe_3O_4 formation	No Fe_3O_4 formation	No Fe_3O_4 formation

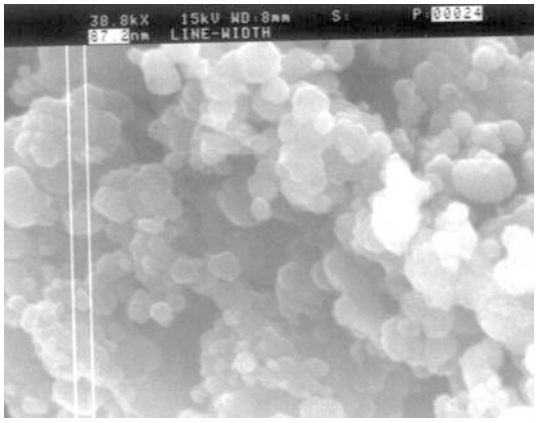

Fig. 4 SEM micrograph obtained with electrosynthesized magnetite (in NaCl electrolyte); 74 nm < $Ø_{observed}$ < 88 nm

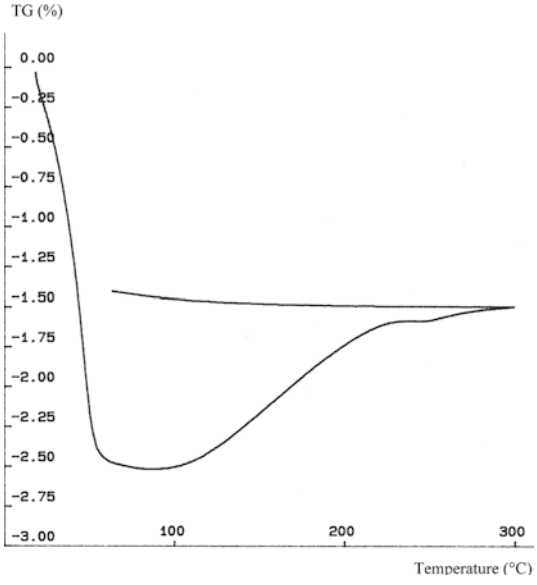

Fig. 5 TGA experiment performed on electrosynthesized magnetite, under air, with a flow rate of 3 °C min^{-1}

$$\left.\begin{array}{ll} \text{Anode :} & Fe + 3OH^- \rightleftharpoons \gamma - FeOOH + H_2O + 3e^- \\ \text{Cathode :} & H_2O + e^- \rightleftharpoons {}^1/_2H_2 + OH^- \\ \text{Solution :} & 3\gamma - FeOOH + {}^1/_2H_2 \rightarrow Fe_3O_4 + 2H_2O \end{array}\right\} \quad (7)$$

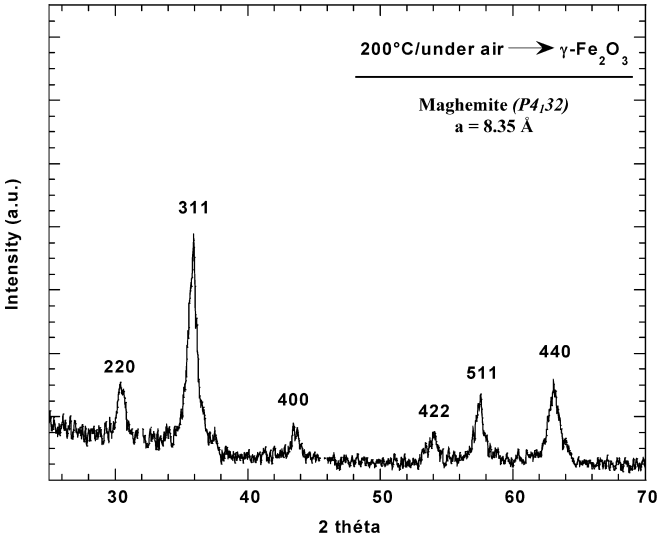

Fig. 6 XRD patterns of magnetite after heating at 300 °C (oxidation to maghemite)

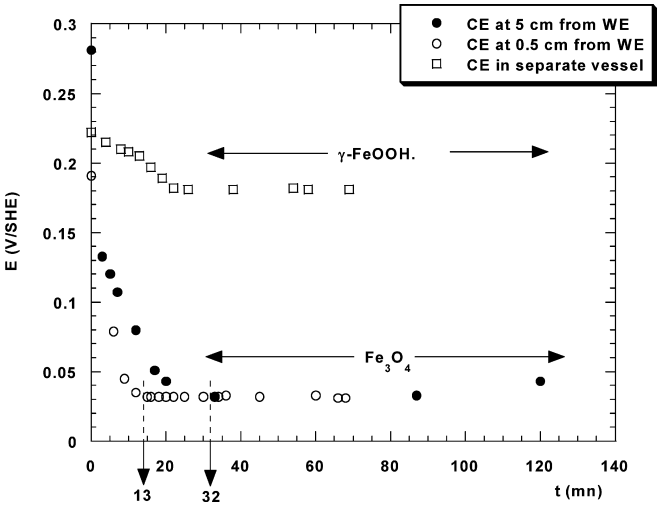

Fig. 7 Influence of the platinum wire position in the cell

The global reaction is then:

$$6Fe + 8H_2O \rightarrow 2Fe_3O_4 + 8H_2 \quad (8)$$

The role of the complexing entities in the electrolytes is purely kinetic. Actually, the charge transfer of the elementary process:

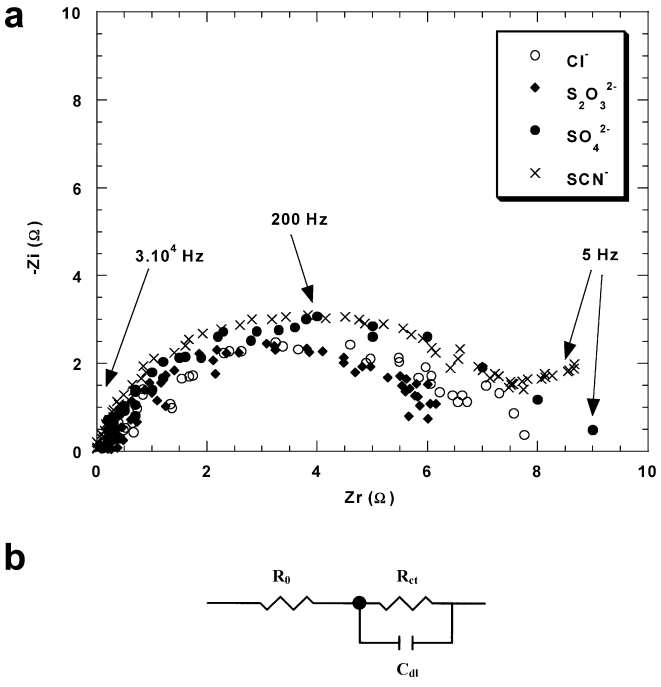

Fig. 8 (**a**) EIS spectra as a function of the complexing species in the electrolyte; (**b**) equivalent electrical circuit modelled to fit the experimental curves

$$\mathrm{Fe} \rightleftharpoons \mathrm{Fe}^{3+} + 3\mathrm{e}^{-} \tag{9}$$

at an iron electrode is known to be very slow ($j_0 = 10^{-8}$ A cm^{-2}) [29, 30]. A way to enhance this electrochemical step is to add complexing agents to the electrolytes in order to decrease the overpotential. Electrochemical impedance spectroscopy (EIS) experiments performed in the different electrolytes are presented in Fig. 8a.

The impedance diagrams show a semi-circle centred on the real axis and characteristic of the electrochemical process at the working electrode: electrolyte resistivity (symbolized by $R_0 \approx$constant$\approx 0.5\ \Omega$) in series with charge transfer (symbolized by R_{ct}) and double layer capacity (symbolized by C_{dl}), both associated in parallel (the equivalent electrical circuit is presented in Fig. 8b). Then, the following equations can be written:

$$C_{\mathrm{dl}} = \frac{1}{2\pi f^{*} R_{\mathrm{ct}}} \tag{10}$$

where f^{*} is the frequency at $-(Z_1)_{\max}$, and:

$$j_0 = \frac{RT}{nFSR_{\mathrm{ct}}} \tag{11}$$

where $RT/F = 26$ mV at 25 °C, n is the number of electrons and S is the electroactive surface. Thiosulfate ions seem to be very interesting since they allow us to make the charge transfer faster ($R_{ct} \approx 5\ \Omega$, i.e. $j_0 \approx 10^{-4}$ A cm^{-2}) than the other complexing species tested ($R_{ct} \approx 10\ \Omega$, i.e. $j_0 \approx 5 \times 10^{-5}$ A cm^{-2}).

It is to be noted that the faster the kinetics, the smaller are the magnetite particles produced (Fig. 3b).

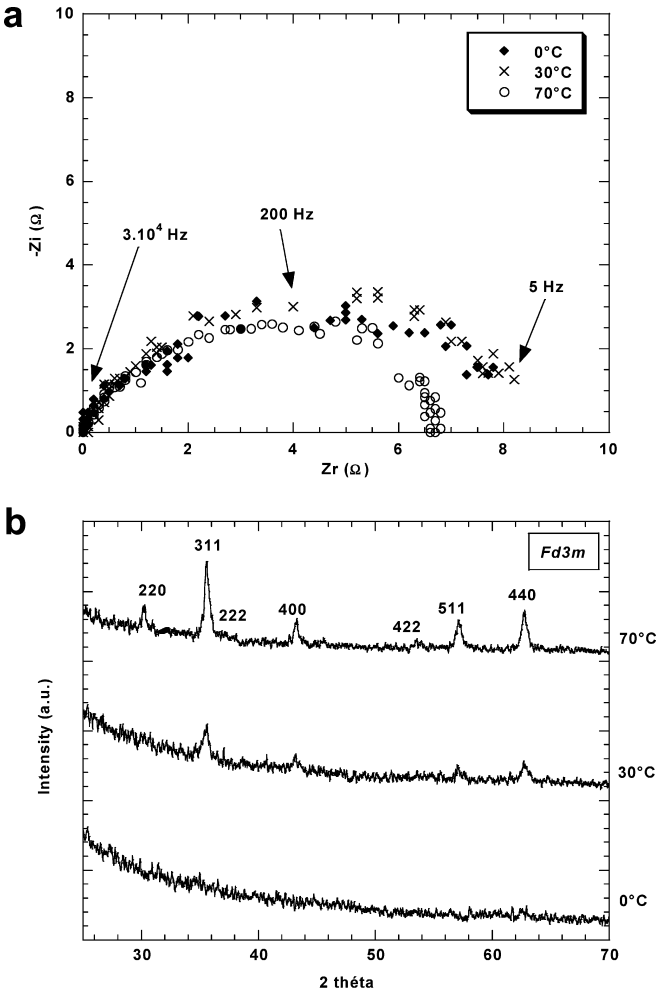

Fig. 9 (**a**) EIS spectra in NaCl electrolyte as a function of the temperature of the cell; (**b**) XRD patterns of the corresponding magnetite particles

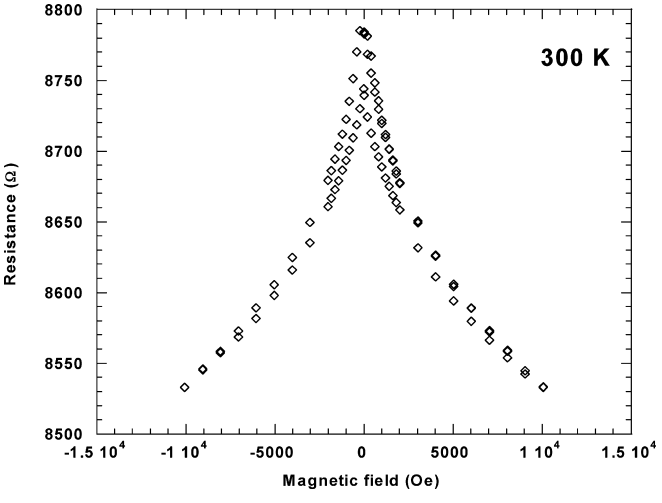

Fig. 10 Magnetoresistance measurements, at 300 K, of pressed magnetite powder, using the four-probe method

However, to be efficient, the complexing species must have a lower affinity for iron(III) ions than hydroxide entities (i.e. p $K_d < 11$), otherwise the

formation of iron oxides in aqueous solution is not possible (because of competitive reactions; this is the case with citrate, whose complexing constant is much too high, p $K_d = 25$).

Another solution to enhance the kinetics is to increase the temperature of the cell. The same EIS experiments have been performed in NaCl electrolyte at 0, 30 and 70 °C (Fig. 9a). The results obtained are quite in line with those expected. The charge transfer is more rapid at higher temperatures, but XRD patterns corresponding to these materials show unambiguously that the higher the temperature of the cell, the larger are the particles produced (Fig. 9b).

There is no interest to increase the heating of the cell if the goal is to keep a small grain size. That is why the research for a good complexing agent is so important. Thiosulfates are very promising compounds for the synthesis of pure nanoscale magnetite particles (Ø≈45 nm).

These results prompted us to evaluate the magnetic behaviour of our small particles. We have measured the magnetoresistance of our Fe_3O_4 material, at room temperature (300 K), under low magnetic fields (≤ 1 T). The curves obtained are presented in Fig. 10. A magnetoresistance of almost 3% is observed in these conditions, which is very promising compared to other experiments that report similar results under more severe conditions (very low temperature, < 120 K, and/or very high magnetic fields, > 5 T) [31, 32, 33].

Conclusions

Details of magnetite electrosynthesis have been developed in this work. The benefit of using complexing agents in the aqueous electrolyte has been demonstrated for both the enhancement of the charge transfer kinetics and the decrease of the grain size to the nanometer level. Indeed, the anodic polarization of a stainless steel electrode, during 30 min under a constant current of 50 mA, allowed us to prepare pure, fine (∼45 nm) and homogeneous magnetite particles, provided the alkaline electrolyte contained complexing thiosulfate ions (0.02 mol L^{-1}).

Acknowledgements The authors are grateful to Mr. Christian Haut (ICMMO, Université Paris Sud – XI), who provided the SEM micrographs of magnetite.

References

1. Elmore WC (1938) Phys Rev 54:309
2. Massart R (1980) CR Acad Sci Paris 291C:1
3. Tronc E, Jolivet J-P, Massart R (1982) Mater Res Bull 17:1365
4. Jolivet J-P, Massart R, Fruchart J-M (1983) Nouv J Chim 7:325
5. Jolivet J-P, Belleville P, Tronc E, Livage J (1992) Clays Clay Minerals 40:531
6. Tronc E, Belleville P, Jolivet J-P, Livage J (1992) Langmuir 8:313
7. Visalakshi G, Venkateswaran G, Kulshreshtha SK, Moorty PN (1993) Mater Res Bull 28:829
8. Siles-Dotor MG, Morales A, Benaissa M, Cabral-Prieto A (1997) Nanostruct Mater 8:657
9. Darken LS, Gurry RW (1946) J Am Chem Soc 68:798
10. Von Osterhont (1975) Magnetic oxides. Wiley-Interscience, New York
11. Konishi Y, Kawamura T, Asai S (1993) Ind Eng Chem Res 32:2888
12. Yitai Q, Yi X, Chuan H, Jing L, Zuyao C (1994) Mater Res Bull 29:953
13. Li Y, Liao H, Qian Y (1998) Mater Res Bull 33:841
14. Chen D, Xu R (1998) Mater Res Bull 33:1015
15. Bae DS, Hau KS, Cho SB, Choi SH (1998) Mater Lett 37:255
16. Fan R, Chen XH, Gui Z, Liu L, Chen ZY (2001) Mater Res Bull 36:497
17. Gabrielli C (1981) Identification of electrochemical processes by frequency response analysis. Solartron, France
18. MacDonald JR (1987) Impedance spectroscopy. Wiley-Interscience, New York, p 84
19. Petzold W, Petzold A (1958) Z Anal Chem 161:241
20. Riegel ER, Schwartz RD (1952) Anal Chem 14:1803
21. Klug HP, Alexander LE (1974) X-ray diffraction procedures for polycrystalline and amorphous materials, 2nd edn. Wiley-Interscience, New York, p 656
22. Dordor P, Marquestant E, Villeneuve G (1980) Rev Phys Appl 15:1607
23. Pourbaix M (1963) Atlas d'équilibres électrochimiques. Gauthier-Villars, Paris
24. Brousse T, Bélanger D (2003) Electrochem Solid-State Lett 6:A244
25. Franger S, Bach S, Pereira-Ramos J-P, Baffier N (2000) Ionics 6:470
26. Franger S, Bach S, Farcy J, Pereira-Ramos J-P, Baffier N (2002) J Power Sources 109:262
27. Pascal P (1963) Nouveau traité de chimie minérale, vol XVI. Masson, Paris
28. Michel A, Bénard J (1964) Chimie minérale. Masson, Paris, p 644
29. Bard AJ, Faulkner LR (1980) Electrochemical methods. Wiley-Interscience, New York
30. Sarrazin J, Verdaguer M (1998) Oxydoréduction. Ellipses, Paris, p 216
31. Wang L, Li J, Ding W, Zhou T, Liu B, Zhong W, Wu J, Du Y (1999) J Magn Magn Mater 207:111
32. Ziese M, Höhne R, Hong NH, Dienelt J, Zimmer K, Esquinazi P (2002) J Magn Magn Mater 242–245:450
33. Hsu J-H, Chen S-Y, Chang C-R (2002) J Magn Magn Mater 242–245:479